

SCIENTIFIC REPORTS



OPEN

Trehalose, sucrose and raffinose are novel activators of autophagy in human keratinocytes through an mTOR-independent pathway

Received: 16 September 2015

Accepted: 06 June 2016

Published: 22 June 2016

Xu Chen^{1,*}, Min Li^{1,*}, Li Li¹, Song Xu¹, Dan Huang¹, Mei Ju¹, Ju Huang², Kun Chen¹ & Heng Gu¹

Trehalose is a natural disaccharide that is found in a diverse range of organisms but not in mammals. Autophagy is a process which mediates the sequestration, lysosomal delivery and degradation of proteins and organelles. Studies have shown that trehalose exerts beneficial effects through inducing autophagy in mammalian cells. However, whether trehalose or other saccharides can activate autophagy in keratinocytes is unknown. Here, we found that trehalose treatment increased the LC3-I to LC3-II conversion, acridine orange-stained vacuoles and GFP-LC3B (LC3B protein tagged with green fluorescent protein) puncta in the HaCaT human keratinocyte cell line, indicating autophagy induction. Trehalose-induced autophagy was also observed in primary keratinocytes and the A431 epidermal cancer cell line. mTOR signalling was not affected by trehalose treatment, suggesting that trehalose induced autophagy through an mTOR-independent pathway. mTOR-independent autophagy induction was also observed in HaCaT and HeLa cells treated with sucrose or raffinose but not in glucose, maltose or sorbitol treated HaCaT cells, indicating that autophagy induction was not a general property of saccharides. Finally, although trehalose treatment had an inhibitory effect on cell proliferation, it had a cytoprotective effect on cells exposed to UVB radiation. Our study provides new insight into the saccharide-mediated regulation of autophagy in keratinocytes.

Trehalose is a natural disaccharide that is found in a diverse range of organisms, such as plants, bacteria, yeast and fungi. By contrast, mammalian cells cannot synthesize trehalose. Trehalose has been reported to have a cytoprotective effect on cells subjected to various stressors, including oxidative damage, dehydration and temperature changes¹. Mitochondria frozen with trehalose have been shown to retain most of their biological properties, such as membrane integrity, ATP synthesis and transmembrane potential². At the molecular level, trehalose has been reported to function as a cryoprotective agent by preventing the crystallization of protein hydration water³. Trehalose treatment can protect the cornea against ultraviolet B (UVB) damage by inhibiting the generation of reactive oxygen and nitrogen species⁴. In *Saccharomyces cerevisiae*, trehalose acts as a free-radical scavenger, thereby decreasing the accumulation of abnormal proteins that arises from oxidative stress-induced damage⁵. Additionally, trehalose prevents the amyloidosis of insulin *in vitro*⁶ and represses β -amyloid aggregation in Alzheimer's disease⁷.

Macroautophagy (hereafter referred to as autophagy) is a cellular degradation process during which double-membrane vesicular structures named autophagosomes are formed and cytosolic components are delivered to the lysosome for breakdown⁸. The autophagy machinery is conserved among eukaryotes from yeast to humans and plays an important role in maintaining cellular homeostasis despite exposure to various types of environmental damage⁹. Abnormal autophagy has been found in many human disorders, including neurodegenerative diseases, metabolic disease, infections and cancer⁸. Accordingly, pharmacological approaches targeted to activate or inhibit autophagy are currently obtaining attention for the treatment of these diseases^{10,11}. Interestingly, trehalose has been identified as an inducer of autophagy in neural cells^{12–14}. Recent studies have

¹Institute of Dermatology, Jiangsu Key Laboratory of Molecular Biology for Skin Diseases and STIs, Chinese Academy of Medical Science & Peking Union Medical College, Nanjing, 210042, China. ²Ontario Cancer Institute, University Health Network, Toronto, Ontario, M5G 2M1, Canada. *These authors contributed equally to this work. Correspondence and requests for materials should be addressed to H.G. (email: doctor_guheng@hotmail.com) or K.C. (email: kunchen181@aliyun.com)

shown that trehalose-induced autophagy has many beneficial effects, such as preventing neural tube defects¹⁵, delaying the progression of amyotrophic lateral sclerosis¹³, ameliorating dopaminergic and tau pathology¹⁶, counteracting cellular prion infection¹⁴ and accelerating the clearance of mutant huntingtin and alpha-synuclein¹².

Mechanistic target of rapamycin (mTOR) is an evolutionarily conserved protein kinase that plays a central role in autophagy regulation and cell growth in response to stress signals, nutritional status and growth factors^{17–19}. Unc-51-like kinase 1 (ULK1) is the substrate of mTOR and is activated when mTOR complex 1 (mTORC1) is inhibited under certain conditions, such as nutrient deprivation or rapamycin treatment²⁰. Consequently, the active ULK1 protein complex triggers autophagy. mTOR complex 2 (mTORC2) is not directly part of the core autophagy machinery. However, mTORC2 has been speculated to be a negative modulator of autophagy because it directly mediates the phosphorylation and thus the activation of the Akt protein, which is a positive regulator of mTORC1¹⁷. Autophagy can also be regulated by mTOR-independent pathways^{21–23}.

The epidermis of mammalian skin is formed through the successive differentiation of keratinocytes and acts as the front-line barrier against biotic, physical and chemical insults²⁴. Recently, autophagy was reported to be involved in keratinocyte cytobiology and pathology, including differentiation²⁵, virus infection²⁶, melanin metabolism²⁷ and the inflammatory response²⁸. Sukserree *et al.*²⁹ reported that mice that are deficient in keratinocyte-specific autophagy-related gene 5 (ATG5, a key protein associated with autophagy), which have inhibited autolysosomal degradation, presented normal cornification-associated cell death. Moreover, Rossiter *et al.*³⁰ found that a significant defect in cornification was not observed in mice that are deficient in keratinocyte-specific ATG7 (a key protein associated with autophagy), which exhibit autophagy suppression in the epidermis, although transepidermal water loss and resistance to penetration of dye were normal in the skin of these mice. These findings indicate that autophagy is not essential for the barrier function of the skin. Interestingly, abnormal presentation of epidermal differentiation was observed in skin grafts of Atg7-deficient mice that had been transplanted onto immunodeficient mice³¹. The epidermis of p18 (a lysosomal adaptor protein)-depleted mice showed severe defects in corneocyte formation and stratum corneum development that were accompanied by the accumulation of autophagosomes and immature lysosomes in the immature corneocyte-like cells. The dysfunction of the fusion between lysosomes and autophagosomes due to p18 ablation led to abnormal development of the mouse epidermis³². Therefore, the actual role of autophagy in keratinocytes needs to be clarified. Because the autophagy machinery is a double-edged sword in many disease conditions, it is important to determine the effects of the activation or inhibition of autophagy. Therefore, inducers or inhibitors of autophagy should be used with caution as disease treatment. Recently, some novel inducers of autophagy, including calcipotriol³³, apigenin³⁴, efavirenz³⁵ and resveratrol³⁶, were identified for keratinocytes. Trehalose has been reported to possess numerous beneficial effects for nervous system diseases via inducing autophagy; however, whether trehalose and other saccharides can activate autophagy in keratinocytes is unknown. Here, we report that treatment with trehalose and other saccharides (sucrose and raffinose) activated autophagy in human keratinocytes and the A431 epidermal cancer cell line through an mTOR-independent pathway. Moreover, trehalose treatment exhibited a cytoprotective effect on cells exposed to UVB radiation, although trehalose treatment itself had an inhibitory effect on cell proliferation.

Results

Trehalose treatment activates autophagy and increases the autophagic flux in HaCaT cells. To monitor the autophagy level, we determined the level of microtubule-associated protein 1 light chain 3 (LC3), which is a widely used protein marker of autophagy¹⁷. The cytosolic form of LC3 (LC3-I) is converted to the phosphatidylethanolamine-conjugated form (LC3-II) when autophagy occurs. In the untreated HaCaT cells (human keratinocyte cell line), we observed basal expression of LC3-I and LC3-II, indicating the basal autophagy level. In a previous study, 100 mM trehalose treatment was reported to increase autophagy in COS-7 cells¹². Therefore, the cells were treated with 50, 100 and 200 mM trehalose for 4, 12 and 24 hours. We found that the conversion of LC3-I to LC3-II was increased in the cells treated with 100 or 200 mM trehalose for 12 or 24 hours (Fig. 1a).

Cellular autophagy is a highly dynamic multi-step process during which sequestered phagophores, autophagosomes and autolysosomes (formed by the fusion of an autophagosome and lysosome) are sequentially formed during autophagic flux. After degradation in the autolysosome, the autophagy process completes the turnover of the autophagosome and its cargo. The inferred LC3-II turnover is used to measure the autophagic flux, by determining the LC3-II level with or without lysosomal blockade (e.g., in the presence of E64d and pepstatin)¹⁷. We observed LC3-II accumulation in the presence of E64d and pepstatin for 12 hours, indicating the basal autophagic flux (Fig. 1b). Moreover, the basal autophagic flux can be inhibited by treatment with the autophagy inhibitor wortmannin (Fig. 1c). Increased LC3-II expression was observed after 100 mM trehalose treatment in the presence or absence of E64d and pepstatin (Fig. 1b). Importantly, this effect was more significant in the presence than in the absence of E64d and pepstatin. This effect was verified using the autophagic blocker chloroquine (Fig. 1d). Rapamycin is a widely used inducer of autophagy in mammalian cells. First, we verified that rapamycin treatment increased the autophagic flux in HaCaT cells. Interestingly, the increased conversion of LC3-I to LC3-II was more significant when the cells were simultaneously treated with rapamycin and trehalose than when the cells were treated with rapamycin or trehalose respectively in the presence of E64d and pepstatin, indicating that trehalose had a synergistic effect on the rapamycin-enhanced autophagic flux (Fig. 1e).

Acridine orange (AO) can be used to stain autophagosomes^{17,37,38}. We found that trehalose treatment increased the red/green fluorescence ratios of HaCaT cells in the absence of E64d and pepstatin, indicating an increase in AO-positive vacuole formation. Moreover, the red/green fluorescence ratios were greater in the presence of E64d and pepstatin than in their absence, indicating blockage of autophagosome degradation. Similar to the results obtained from the LC3-II turnover assay, we observed a more significant accumulation of AO-positive vacuoles after trehalose treatment in the presence of protease inhibitors (Fig. 1f).

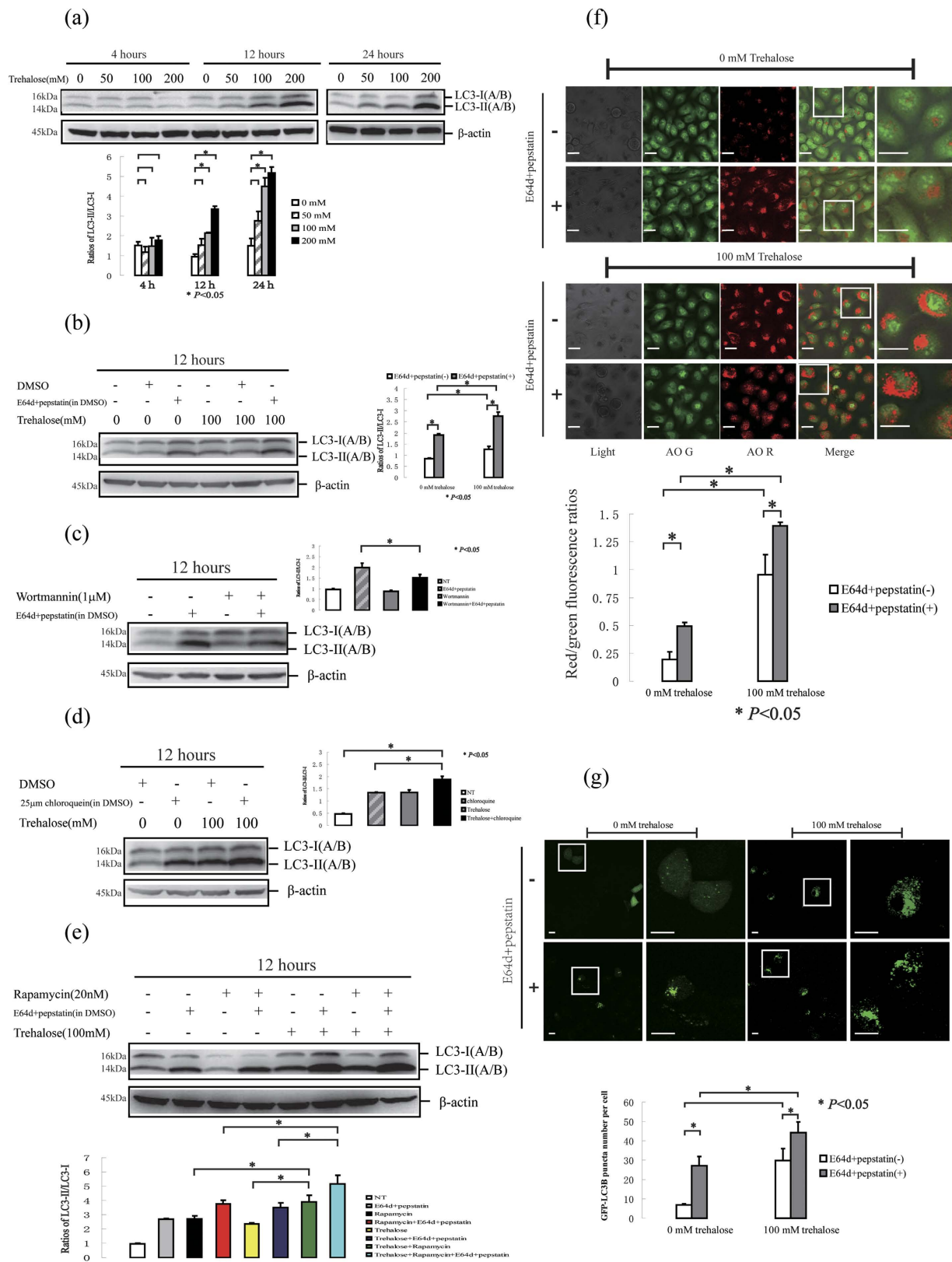


Figure 1. (a) HaCaT cells were treated with or without different doses of trehalose for indicated hours. Similar results to (a) were repeated in five different passages of cells. (b) HaCaT cells were treated with or without 100 mM trehalose for 12 hours in the presence or absence of E64d and pepstatin. 0.01% DMSO (equity for E64d and pepstatin solutions) was used as solvent control. Statistical difference of LC3-II/LC3-I ratios was not observed between the DMSO-treated and untreated cells. (c) HaCaT cells were treated with or without 1 μ M wortmannin for 12 hours in the presence or absence of E64d and pepstatin. (d) HaCaT cells were treated with or without 100 mM trehalose for 12 hours in the presence or absence of chloroquine. (e) HaCaT cells were treated

with or without 100 mM trehalose and rapamycin for 12 hours in the presence or absence of E64d and pepstatin. (f) HaCaT cells were treated with or without 100 mM trehalose for 12 hours. Then, cells were incubated with AO. (g) HaCaT cells were pretreated with or without GFP-LC3B before trehalose co-treatment for 12 hours. The cells were imaged using a laser scanning confocal microscope, and the means of red/green fluorescence ratios or GFP-LC3 puncta for individual cells were determined for statistical analysis. The data were shown as means \pm SD of three independent experiments and representative figures were shown. Bars = 20 μ m.

The GFP-LC3B (the LC3B protein tagged at its N terminus with a green fluorescent protein (GFP)) assay was used to monitor autophagy through fluorescence microscopy by measuring punctate GFP fluorescence³⁹. Consistent with the AO staining results, trehalose treatment increased the number of GFP-LC3B puncta in the cells. E64d and pepstatin incubation induced more GFP-LC3B puncta in the trehalose-treated cells than in the cells without lysosomal blockade, indicating the accelerated conversion of LC3-I to LC3-II (Fig. 1g).

These findings strongly suggest that trehalose treatment increases the autophagic flux in HaCaT cells.

Trehalose treatment induces autophagy of HaCaT cells via an mTOR-independent mechanism.

Trehalose has been reported to be an mTOR-independent autophagic enhancer in cells of the nervous system^{12,40}. Here, we confirmed that the activities of mTORC1 and mTORC2 were not affected in trehalose-treated HaCaT cells. We found that the phosphorylation levels of mTOR and regulatory-associated protein of mTOR (Raptor, a component of mTORC1) were not affected by trehalose treatment. The phosphorylation levels of the mTORC1 substrate 4E-BP1⁴¹ at Thr37/46 and Ser65 were also not affected. In addition, trehalose treatment did not affect the phosphorylation of the rapamycin-insensitive companion of mTOR protein (Rictor, a core component of mTORC2⁴²) at Thr1135 or of protein kinase C α (PKC α , a substrate of the mTORC2 kinases; mTORC2 facilitates its phosphorylation) at Thr638 (Fig. 2a). Rapamycin-induced autophagy is mediated by an mTOR-dependent mechanism. Therefore, we monitored whether mTOR activity was affected upon trehalose treatment in the presence or absence of rapamycin. In the rapamycin-treated cells, the mTOR phosphorylation levels were decreased and the 4E-BP1, p70 S6 kinase (another important substrate of the mTOR kinase) and S6 ribosomal protein (substrate of the p70 S6 kinase) activities were inhibited, indicating the inhibition of mTOR signalling. However, these results were not observed in the trehalose-treated cells. Interestingly, the inhibition of mTOR activity was observed in cells treated with trehalose and rapamycin together, indicating that trehalose did not affect the rapamycin-induced inhibition of mTOR signalling (Fig. 2c). These findings suggest that trehalose-enhanced autophagy is mediated via an mTOR pathway.

A series of genes reported to be involved in the molecular cellular autophagy machinery have been denoted the autophagy-related genes (ATG). In our study, we determined the unc-51-like kinase 1 (ULK1, yeast ATG1 homologue), ATG3, ATG5, ATG7, ATG9A, Beclin 1, WIPI2 and WIPI1 (yeast ATG18 homologue) protein levels in trehalose-treated HaCaT cells. These proteins were not affected by trehalose treatment. The phosphorylation of ULK1 at Ser555 and Ser757 was also not changed (Fig. 2b,d). These findings indicate that these ATG proteins may not be involved in the autophagic machinery of keratinocytes via regulating the protein levels. In some settings, p62 can be used as a protein marker to monitor autophagy in addition to LC3. However, we did not observe a change in the p62 protein level in the trehalose-treated HaCaT cells (Fig. 2b). Finally, we determined the p62 protein level in human keratinocytes treated with rapamycin or a lysosomal inhibitor (Fig. S1c–e). Our findings verified the conclusion that there was not always a clear correlation between the LC3-II increase and p62 decrease¹⁷.

Torin 1 and pp242 are mTOR inhibitors^{43,44}. We found that torin 1 and pp242 both inhibited mTOR activity and subsequently caused an increase in the conversion of LC3-I to LC3-II. Moreover, inhibition of mTOR activity was observed in cells treated with torin 1 or pp242 in the presence or absence of trehalose (Fig. 2e). In agreement with the assay in the cells treated with rapamycin and/or trehalose, these findings demonstrate that mTOR signalling in HaCaT cells was sensitive to the mTOR inhibitors but was not affected by trehalose treatment.

Trehalose, sucrose and raffinose activate mTOR-independent autophagy in HaCaT cells.

To investigate whether the trehalose-induced autophagy was caused by osmotic stress, we monitored the autophagy level in HaCaT cells treated with 100 mM of the disaccharide sucrose or maltose for 12 hours. Sucrose treatment increased the conversion of LC3-I to LC3-II, the red/green fluorescence ratios in the AO-stained cells and the GFP-LC3 puncta, indicating autophagy induction. In contrast, a similar effect was not observed in the maltose-treated cells, suggesting that the induction of autophagy was not caused by osmotic stress and was not a general property of disaccharides. Additionally, a 100 mM dose of glucose (monosaccharide) or sorbitol (sugar alcohol) did not induce autophagy. Interestingly, we found that raffinose (trisaccharide) treatment increased the conversion of LC3-I to LC3-II, the red/green fluorescence ratios in the AO-stained cells and the GFP-LC3 puncta, indicating that raffinose induced autophagy (Fig. 3a–c). Moreover, the sucrose or raffinose treatments increased the autophagic flux (Fig. 3d).

The mTORC1, mTORC2 and ULK1 activities were not affected by trehalose, sucrose or raffinose treatment. Interestingly, phosphorylation of the S6 ribosomal protein was decreased in cells treated with sucrose or raffinose, suggesting that these saccharides affected mRNA translation in the HaCaT cells (Fig. 3d,e).

Trehalose treatment induces autophagy in human primary keratinocytes and the A431 epidermal cancer cell line.

We monitored the autophagy levels in other human keratinocytes treated with trehalose, including primary keratinocytes, keratinocytes transformed with human papillomavirus 16 (HPV-16) E6/E7 (CCD 1102 KERTr cells), as well as the A431 epidermal cancer cell line⁴⁵ and the HeLa human cervical carcinoma cell line. We found that 100 mM trehalose treatment for 12 hours increased the autophagy levels in these

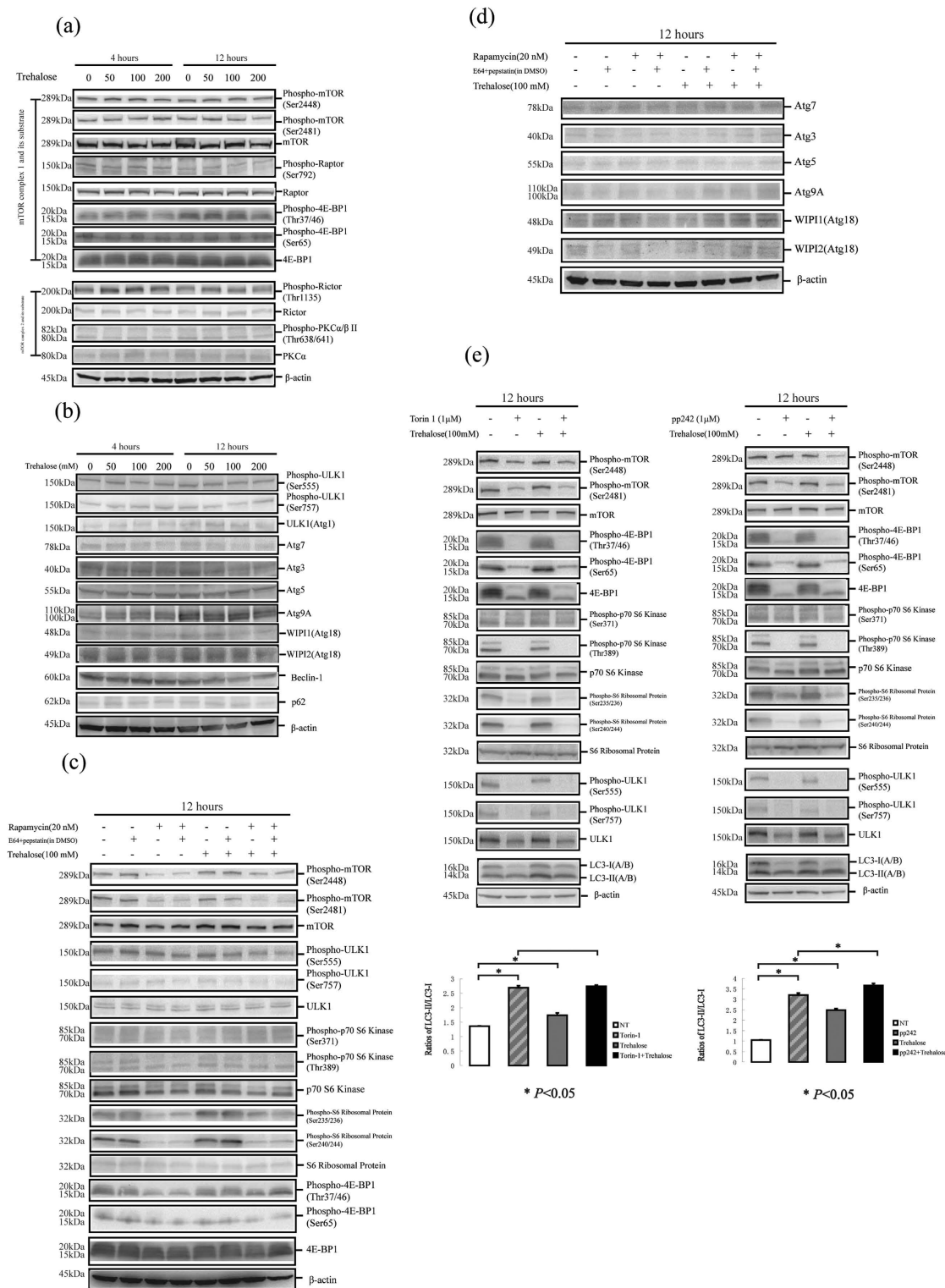


Figure 2. HaCaT cells were treated with or without different doses of trehalose (50, 100 or 200 mM) for 4 or 12 hours. **(a)** Western blotting analysis was performed using primary antibodies against mTOR, phospho-Ser2448 mTOR, phospho-Ser2481 mTOR, Raptor, phospho-Ser792 Raptor, 4E-BP1, phospho-Thr37/46 4E-BP1, phospho-Ser65 4E-BP1, Rictor, phospho-Thr1135 Rictor, Phospho-Thr638/641 PKCα/β or PKCα. **(b)** Western blotting analysis was performed using primary antibodies against ULK1, phospho-Ser555 ULK1, phospho-Ser757 ULK1, ATG7, ATG5, ATG3, ATG9A, WIP1 or WIP2. HaCaT cells were treated with or without 100 mM trehalose and rapamycin for 12 hours in the presence or absence of E64d and pepstatin. Then, the activities of mTORC1, ULK1, S6 ribosomal protein phosphorylation **(c)** and ATG proteins **(d)** were determined by western blotting using the indicating primary antibodies. β-actin served as a loading control. Representative figures were shown from three independent experiments.

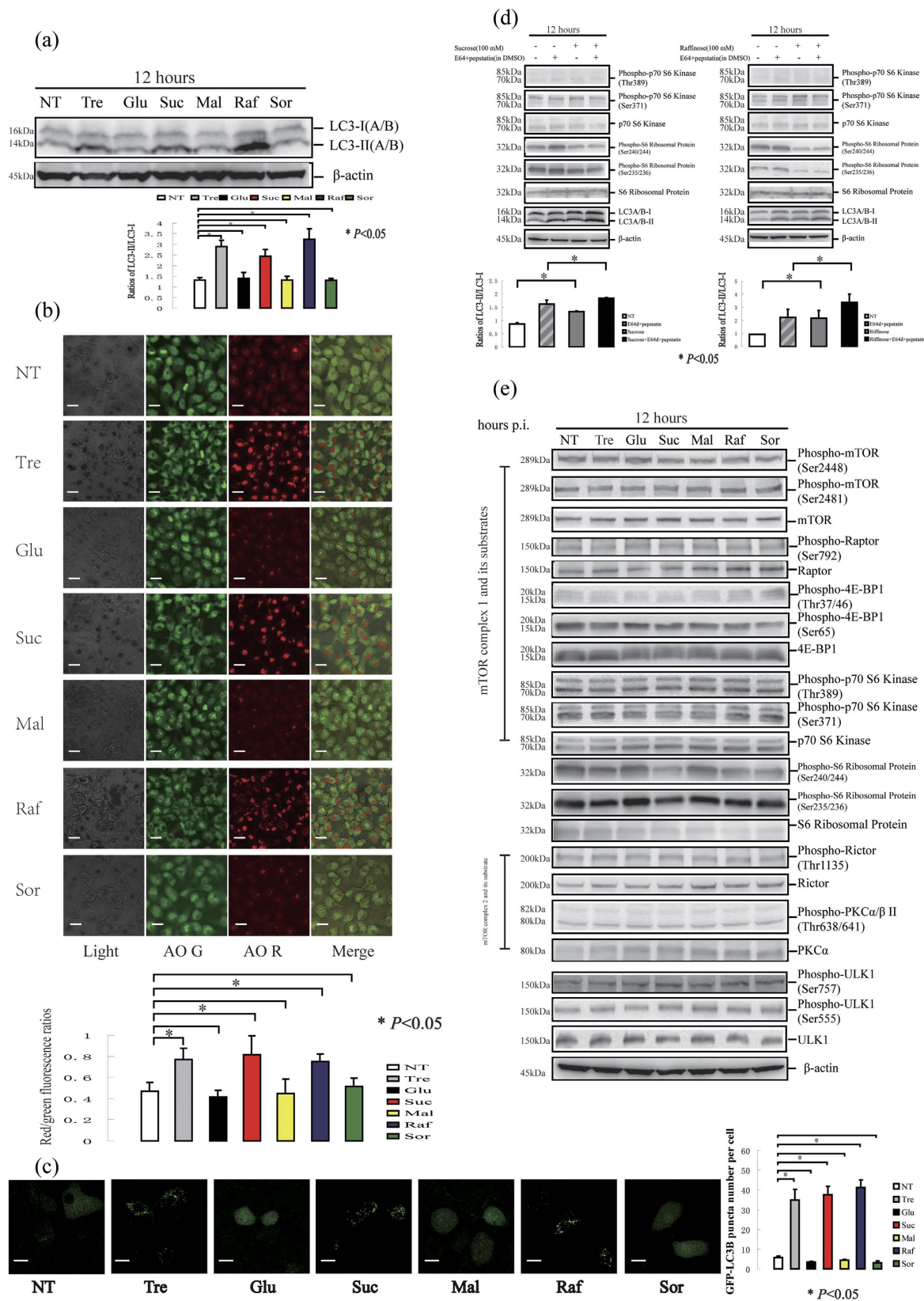


Figure 3. HaCaT cells were treated with or without trehalose (Tre), glucose (Glu), sucrose (Suc), maltose (Mal), raffinose (Raf) or sorbitol (Sor) at the same dose of 100 mM for 12 hours. (a) Expression of LC3 protein was determined by western blotting, and then ratios of LC3-II/LC3-I was calculated. β -actin served as a loading control. (b) The means of red/green fluorescence ratios for individual cells with or without above saccharides treatment were determined in three independent experiments of AO staining assay. (c) HaCaT cells were pretreated with GFP-LC3B before co-treatment of above saccharides for 12 hours. Then, GFP-LC3 puncta

per cell was quantified. The cells were imaged using a laser scanning confocal microscope. (d) HaCaT cells were treated with or without sucrose or raffinose respectively in the presence or absence of E64d and pepstatin, and the levels of LC3, p70 S6 kinase and S6 ribosomal protein were determined by western blotting. (e) HaCaT cells were treated with above saccharides respectively and then the activities of mTORC1, mTORC2, ULK1 and S6 ribosomal protein were determined. β -actin served as a loading control. The data were shown as means \pm SD of three independent experiments, and representative figures were shown. Bars = 20 μ m.

cells with the exception of the HeLa cells (Fig. 4a–d). The mTORC1 and mTORC2 activities were not affected by trehalose treatment in these cells (with the exception of the A431 cells) regardless of whether autophagy was activated. In the trehalose-treated A431 cells, we observed that the phosphorylation of the p70 S6 kinase (an mTOR substrate) and the S6 ribosomal protein was decreased, whereas the phosphorylation of mTORC1 and another substrate (4E-BP1) was not affected. These findings demonstrate the specificity of p70 S6 kinase activity in A431 cells compared with normal keratinocytes. Furthermore, ULK1 activity and some ATG proteins were not affected in the cells treated with trehalose (Fig. 5a,b).

Autophagy induction was observed in the HeLa cells when the trehalose incubation time was lengthened to 24 hours, indicating that the HeLa cells were likely to be insensitive to brief treatment with trehalose (Fig. 6a). Indeed, Sarkar *et al.* reported that autophagy was induced in HeLa cells treated with 100 mM trehalose for 24 hours¹². Moreover, autophagy in the HeLa cells was induced by treatment with sucrose or raffinose (Fig. 6c–e). Importantly, autophagy induction in the HeLa cells treated with trehalose, sucrose or raffinose was mediated via an mTOR-independent way (Fig. 6a–c).

Trehalose treatment exhibits a cytoprotective effect on cells exposed to UVB radiation. In this study, cell viability was examined using the LDH assay and trypan blue staining, and cell proliferation was detected using the colony formation assay (the methodology was based on references^{46–48}). The LDH assay data showed that trehalose treatment for 4, 12, 24 or 48 hours slightly increased LDH release at a stable low level, whereas a 50 mJ/cm² UVB treatment led to an increase in LDH release in a time-dependent manner, with the most significant effect observed 48 hours after exposure. Interestingly, although trehalose treatment only slightly increased LDH release, it significantly attenuated UVB-induced LDH release 48 hours after exposure but had no significant effect 12 to 24 hours after exposure. Furthermore, the trypan blue staining results showed that UVB radiation significantly increased the number of trypan blue-stained cells, whereas this effect was not observed in the trehalose-treated cells. Trehalose treatment for 12 or 24 hours after UVB exposure recovered the increase in the UVB-treated cells stained with trypan blue.

The LDH assay and trypan blue staining results described above demonstrated that trehalose treatment exhibited a cytoprotective effect on cells exposed to UVB damage (Fig. 7a,b), whereas the colony formation assay results showed that trehalose failed to recover the cell proliferation damage in the UVB-treated cells. First, our data showed that trehalose treatment for 12 hours decreased colony formation, suggesting an inhibitory effect on cell proliferation. Moreover, we did not observe any cell colony formation in the 50 mJ/cm² UVB-treated cells with or without trehalose treatment, indicating that this dose of UVB treatment severely decreased cell proliferation (Fig. 7c).

Interestingly, we found that low doses of UVB (5 or 10 mJ/cm²) treatment also decreased ‘normal’ colony formation (>20 cells per colony) and increased ‘excessive’ colony formation, resulting in an increase in the huge colonies (>200 cells). These findings demonstrate that the low dose of UVB stimulation not only impairs normal cell proliferation but also induces ‘undisciplined’ cell proliferation in some surviving cells after UVB exposure. In fact, we detected a low level of ‘excessive’ colony formation in cells under normal culture conditions, and that was decreased by trehalose treatment. Furthermore, trehalose treatment prohibited the increase in ‘excessive’ colony formation caused by 5 or 10 mJ/cm² UVB radiation. These data suggest that the cytoprotective effect of trehalose in the UVB-challenged HaCaT cells reflects the prevention of abnormal excessive proliferation.

Next, we found that 50 mJ/cm² UVB radiation led to more significant cleavage of caspase-3 and PARP than the 10 and 75 dose exposures. Caspase-3 and PARP cleavage was maintained at a stable level after 4, 12 and 24 hours of 50 mJ/cm² UVB exposure; their cleavage levels 12 hours post-radiation were slightly higher than the levels detected at 4 and 24 hours (Fig. 7d,e). In the 50 mJ/cm² UVB-treated cells, the ratio of cells stained with Annexin and PI was also increased 12 hours post-exposure (Fig. 7f,g), suggesting that UVB triggered apoptosis. Interestingly, the increase in cleaved caspase-3, cleaved PARP and cells stained with Annexin and PI 12 hours after 50 mJ/cm² UVB stimulation was not affected by trehalose treatment. We confirmed that the 50 mJ/cm² UVB-induced cleavage of caspase-3 and PARP 24 hours post-exposure was also not affected by trehalose treatment (Fig. 7f,h).

We found that trehalose treatment increased autophagy in HaCaT cells with or without UVB exposure compared with trehalose-untreated cells (Fig. 7f,g).

In conclusion, trehalose treatment had both an inhibitory effect on cell proliferation and a cytoprotective effect on cells exposed to UVB radiation. However, the apoptosis triggered by treatment with 50 mJ/cm² UVB was not affected by trehalose treatment.

Discussion

Here, we reported that trehalose, sucrose and raffinose were novel mTOR-independent inducers of autophagy in human keratinocytes. Interestingly, this effect is not common to other saccharides.

Autophagy has been strongly implicated in human skin diseases, although limited findings have been reported. First, genetic polymorphisms of some ATG genes have a close relationship with skin diseases. Douroudis *et al.*

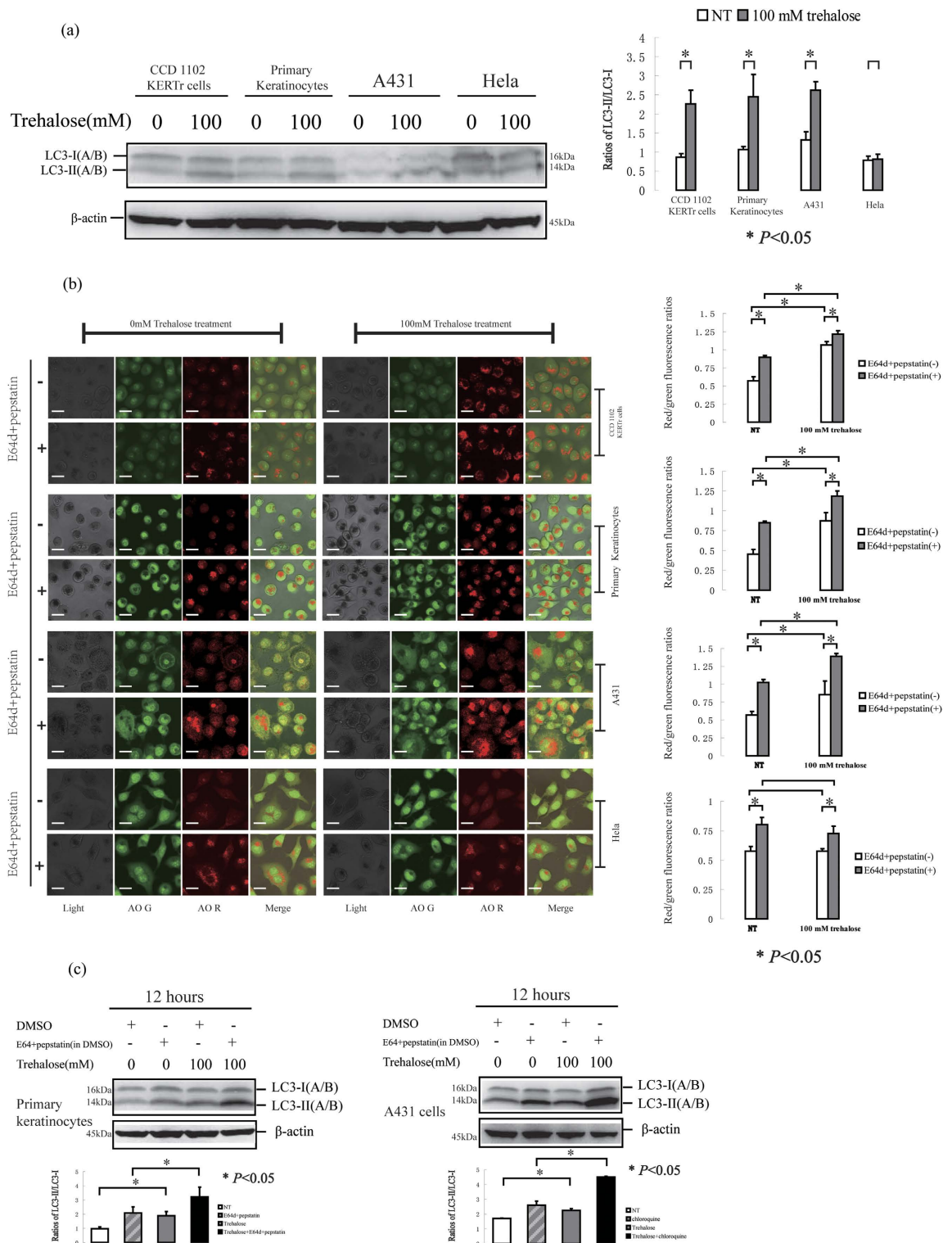


Figure 4. CCD 1102 KERTr cells (keratinocytes transformed HPV 16 E6/E7 oncogenes), human primary keratinocytes, A431 cells and HeLa cells were treated with 100 mM trehalose for 12 hours. (a) The expression of LC3 protein was determined by western blotting, and then the ratios of LC3-II/LC3-I was calculated for statistical analysis. β -actin served as a loading control. The cells were imaged for AO staining assay using a laser scanning confocal microscope. (b) The means of red/green fluorescence ratios for individual cells in three independent experiments were determined. (c) Human primary keratinocytes or A431 cells were treated with or without 100 mM trehalose in the presence or absence of E64d and pepstatin. The levels of LC3 protein were determined by western blotting, and the ratios of LC3-II/LC3-I was calculated. β -actin served as a loading control. The data were shown as means \pm SD of three independent experiments, and representative figures were shown. Bars = 20 μ m.

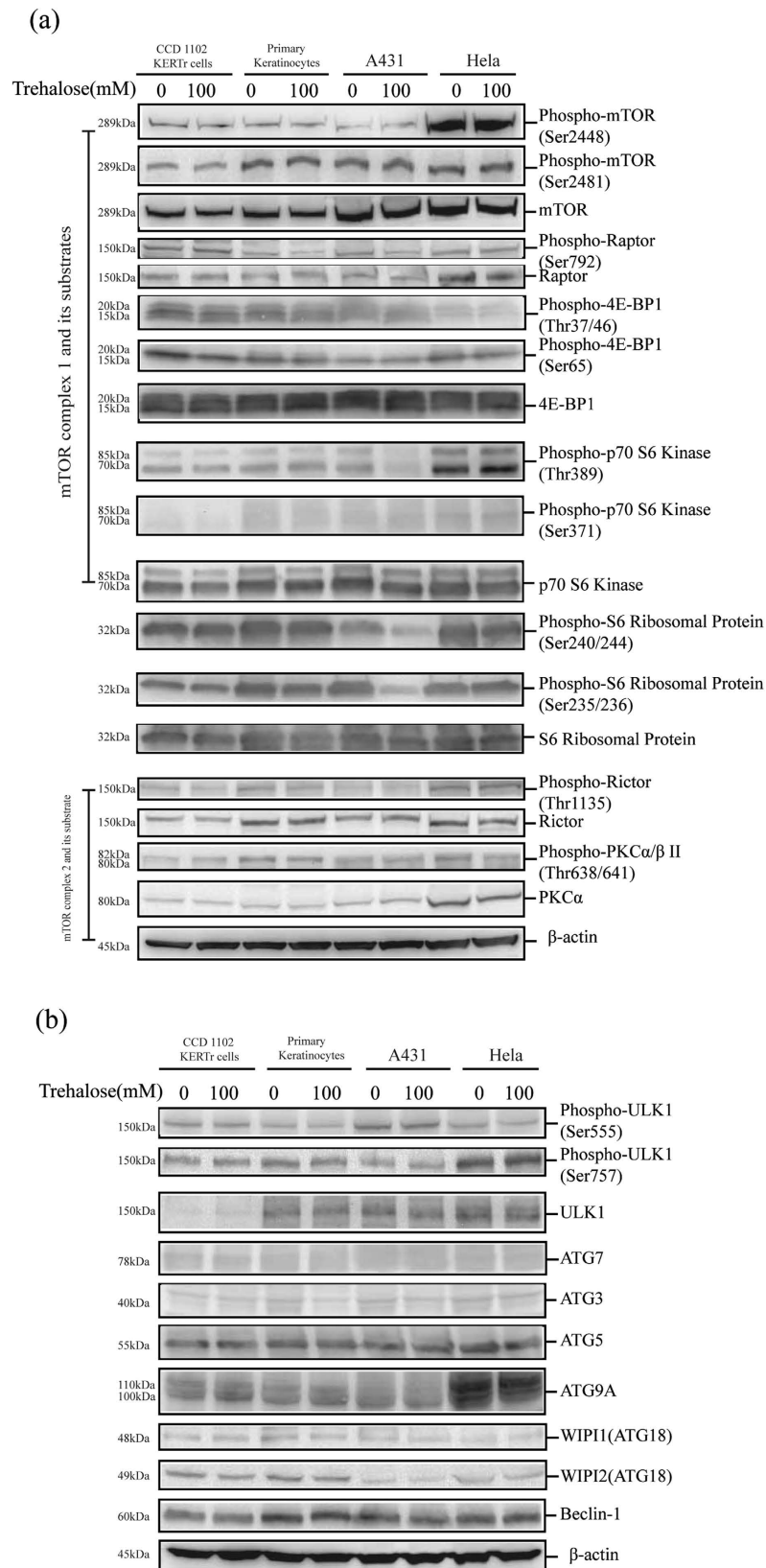


Figure 5. CCD 1102 KERTr cells (keratinocytes transformed HPV 16 E6/E7 oncogenes), human primary keratinocytes, A431 cells and HeLa cells were treated with 100 mM trehalose for 12 hours. Western blotting analysis was performed to determine the activities of mTORC1, mTORC2 and S6 ribosomal protein (a) and the levels of ATG proteins (b) using indicated primary antibodies. β -actin served as a loading control. Representative figures were shown from three independent experiments.

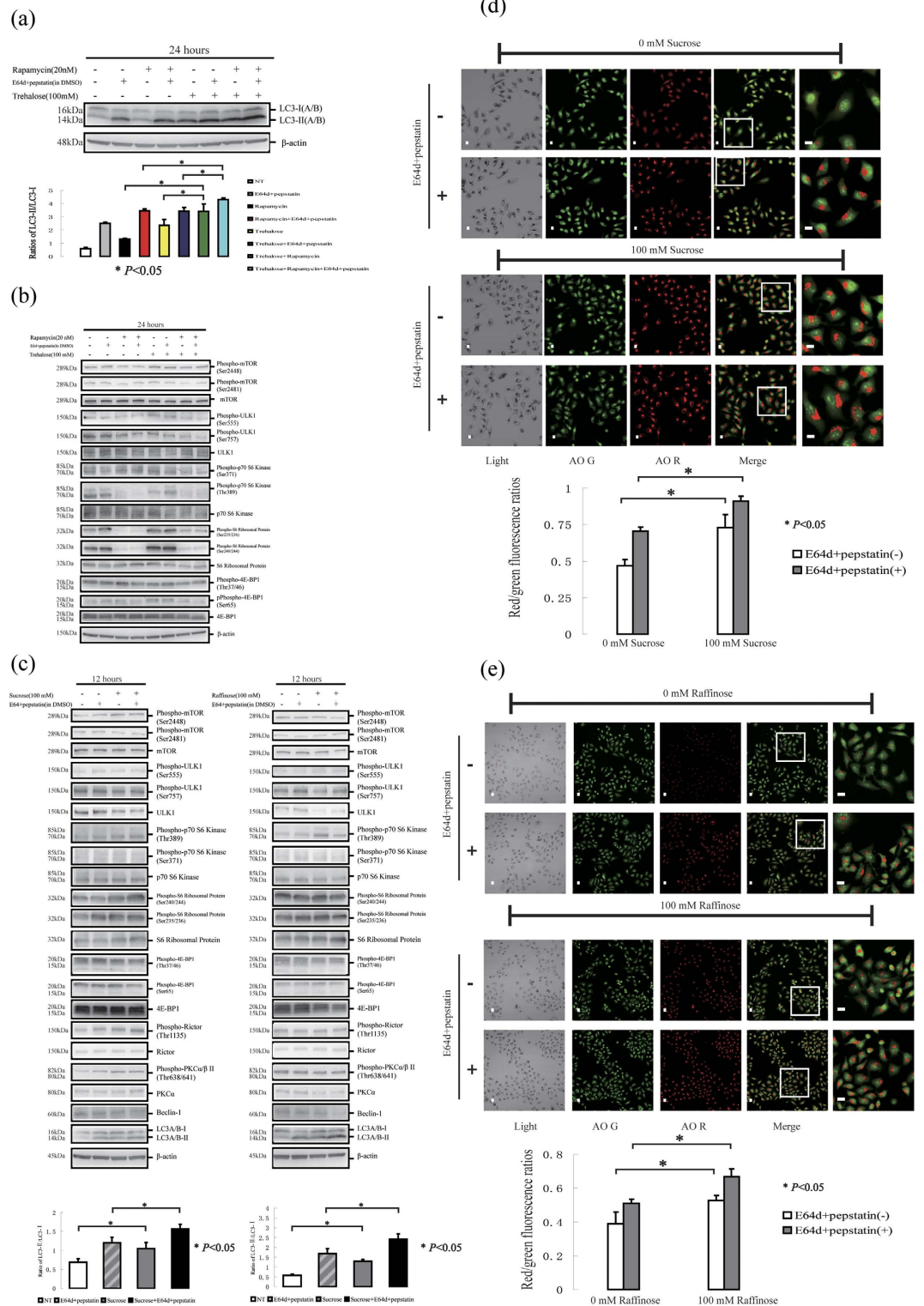


Figure 6. (a) HeLa cells were treated with or without 100 mM trehalose and rapamycin for 24 hours in the presence or absence of E64d and pepstatin. The level of LC3 protein was determined by western blotting, and then ratios of LC3-II/LC3-I was calculated. (b) Then, activities of mTORC1, ULK1 and S6 ribosomal protein were determined by western blotting. β-actin served as a loading control. HeLa cells were treated with or without sucrose or raffinose in the presence or absence of E64d and pepstatin. (c) Western blotting was performed to determine the conversion of LC3-I to LC3-II and activities of mTORC1, mTORC2, ULK1 and S6 ribosomal protein. Additionally, the cells were imaged for AO staining assay using a laser scanning confocal microscope (d,e). The means of red/green fluorescence ratios for individual cells were determined in three independent experiments of AO staining. The data were shown as means ± SD of three independent experiments, and representative figures were shown. Bars = 20 μm.

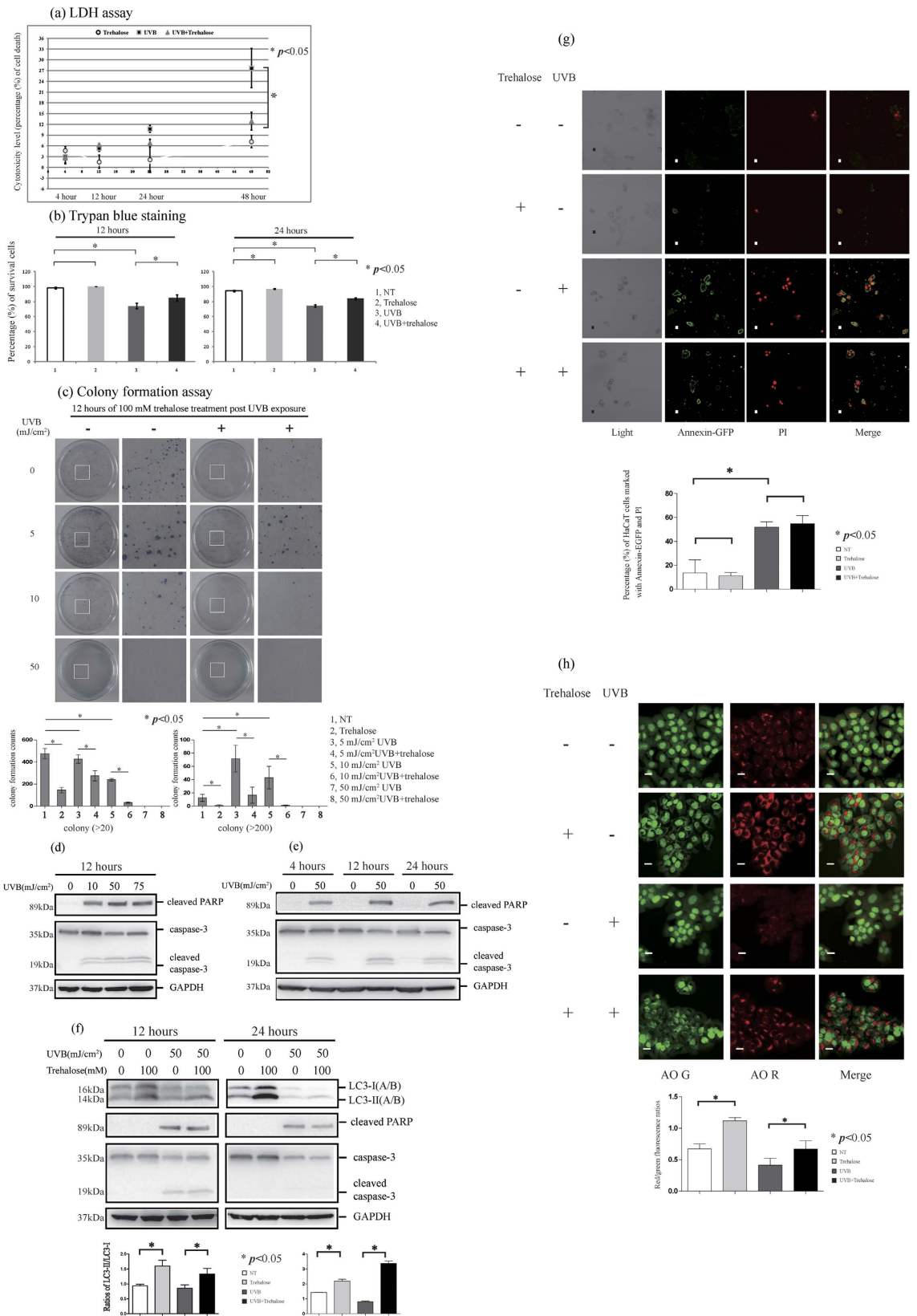


Figure 7. HaCaT cells were treated with or without 50 mJ/cm² UVB radiation, and then the cells were cultured in the presence or absence of 100 mM trehalose for 4, 12, 24 and 48 hours respectively. Supernatants of the cells culture medium were performed by LDH assay (A). Cytotoxicity level values (percentage of cell death) were shown as means \pm SD of three independent experiments. HaCaT cells were treated with or without 50 mJ/cm² UVB radiation, and then the cells were cultured in the presence or absence of 100 mM trehalose. Then, the cells were performed by trypan blue staining (B) or by colony formation assay (C). The percentages of

survival cells (B) or colony formation counts (C) were shown as means \pm SD of three independent experiments. (D–F) Western blotting was used to determine the levels of apoptosis molecular markers (cleaved PARP and caspase-3) and LC3 protein. The cells were imaged for AO staining assay or Annexin V-EGFP apoptosis detection using a laser scanning confocal microscope. The percentages of HaCaT cells marked with Annexin-EGFP and PI were calculated (G). The means of red/green fluorescence ratios for individual cells were determined (H). The means \pm SD represented from three independent experiments, and representative figures were shown. Bars = 20 μ m.

reported that polymorphisms in the key ATG gene ATG16L1 are associated with psoriasis vulgaris⁴⁹ and palmoplantar pustulosis⁵⁰. Jeong *et al.* reported that polymorphisms of the UVRAG gene, which participates in the autophagy machinery through its interaction with Beclin 1, are associated with susceptibility to non-segmental vitiligo in a Korean sample⁵¹. Second, autophagy activity may contribute to the epidermal defence against virus infection. Varicella zoster virus (VZV) and herpes simplex virus (HSV) are common pathogens in human skin disorders. Buckingham *et al.* reported that autophagosomes were abundant in transplanted infected skin tissues in a mouse model of VZV pathogenesis. Moreover, autophagy in a VZV-infected cell was significantly distinct from that in an HSV-infected cell⁵². Grose also reported that autophagosomes were observed early in the cells at the base of the cutaneous vesicles caused by VZV infection⁵³. Importantly, autophagy has been discovered to play a crucial role in skin cancer, although these reports are extremely rare compared with investigation on tumours of other organs. For example, LC3A-positive 'stone-like' structures have been detected in cutaneous squamous cell carcinomas (SCC), indicating that the autophagic activity in SCC may serve as an indicator of tumour aggressiveness⁵⁴. Furthermore, the autophagy inhibitor 3-MA has been shown to enhance sensitivity to 5-FU-induced chemotherapy⁵⁵.

Tong *et al.* reported that apigenin induces keratinocyte autophagy through an mTOR-dependent pathway and is associated with the activation of the AMP-activated protein kinase (AMPK)³⁴. Dong *et al.* found that efavirenz triggered keratinocyte autophagy, which was accompanied by a decrease in mTOR phosphorylation and ERK activation³⁵. These findings suggest that mTOR plays an important role in autophagy activation in keratinocytes. However, mTOR was not involved in autophagy induction in keratinocytes in response to trehalose, sucrose and raffinose treatment. In contrast with these reported inducers, our findings demonstrate that the autophagy machinery is complex and diverse in human keratinocytes.

Trehalose is a type of disaccharide that consists of two glucose molecules connected through an α , α -1,1-glycosidic linkage. Trehalose is not easily hydrolysed by acid, and glucosidase is not able to cleave its glycosidic bond¹. However, periplasmic trehalase can catalyse trehalose to hydrolyse trehalose into glucose under high osmolarity conditions; then, the glucose is utilized by the phosphotransferase system for glycolysis in *Escherichia coli*⁵⁶. Otherwise, glucose can also be transformed into trehalose through an acid reversion⁵⁷. If trehalose is not stable in the keratinocyte culture environment and consequently is converted to glucose, autophagy may be induced by the high glucose level. Therefore, we confirmed that 100 mM glucose did not trigger autophagy. The results suggest that the trehalose-induced autophagy may not be caused by the increase in the glucose level generated from trehalose. Interestingly, an increased intracellular glucose concentration has been reported to induce autophagy via an mTOR-dependent pathway in COS-7 cells⁵⁸ or via the ERK pathway in the chick embryo⁵⁹. However, our data indicate that high-level glucose treatment cannot trigger keratinocyte autophagy. Spravchikov *et al.* found that the phosphorylation of insulin-like growth factor receptor decreased when keratinocytes were cultured under high glucose conditions, thereby inhibiting glucose uptake⁶⁰. We speculate that cells derived from different tissues have distinct abilities to uptake external glucose and that human keratinocytes can prohibit the increase in the intracellular glucose concentration under high-level glucose culture conditions. Therefore, the high level of glucose did not trigger keratinocyte autophagy. Importantly, DeBosch *et al.*⁶¹ reported that trehalose treatment inhibits members of the SLC2A (also known as GLUT) family of the glucose transporters and that trehalose-mediated glucose transport inhibition induces AMPK-dependent autophagy in murine hepatocytes. Therefore, more studies are needed to investigate the signalling pathway associated with glucose transport and metabolism in trehalose-treated cells.

Sucrose and trehalose are both non-reducing disaccharides that possess similarities in synthesis and function. Interestingly, when these oligosaccharides are maintained at a high concentration, cells are more resistant to various stressors, such as oxidative stress, heat and dehydration⁶². Raffinose is an oligosaccharide that can accumulate in some plant cells, which may afford considerable resistance against stresses⁶². Interestingly, Seglen *et al.*^{63,64} reported that sucrose and raffinose could accumulate in the cytoplasm and sequester in the autophagosome in mammalian cells. Indeed, radiolabelled sucrose and raffinose are good probes in autophagy studies^{63,65}. Recently, Higuchi *et al.* reported that sucrose induced the accumulation of sucrose-containing vesicles and autophagy in mouse embryonic fibroblasts⁶⁶. Here, we verified that keratinocyte autophagy was enhanced by sucrose or raffinose treatment. We speculate that keratinocytes promote autophagy to degrade the redundant sucrose or raffinose when these saccharides cannot be utilized after a certain amount of uptake. However, whether trehalose is also the cargo of autophagosomes has not been elucidated.

UVB is radiation at 280–320 nm, in the natural ultraviolet band of the spectrum and is associated with skin conditions such as sunburn and photocarcinogenesis^{48,67,68}. Many studies have reported that various natural agents (e.g., epigallocatechin gallate⁶⁹, pomegranate polyphenol extract⁷⁰, and resveratrol³⁶) have photoprotective effects against UV injury. Importantly, Vitale *et al.* found that the anti-photodamage effect of resveratrol was related to the induction of keratinocyte autophagy³⁶, suggesting that autophagy regulation was a potential target of photoprotection. Our study indicates that trehalose may be considered as a potential anti-photodamage agent. Importantly, trehalose had an inhibitory effect on the abnormal cell proliferation induced by UVB stimulation.

UVB is an important apoptotic trigger for keratinocytes⁷¹ and the apoptosis mechanism plays a crucial role in prohibiting photocarcinogenesis through the removal of the precancerous cells generated by UV damage⁷². Moreover, there is close interplay between autophagy and apoptosis. For instance, GADD34, which is a protein expressed following DNA damage, suppresses apoptosis in macrophages through enhancement of autophagy⁷³. Our findings suggest that the apoptotic molecular markers cleaved caspase-3 and PARP were distinct following different doses of UVB exposure, suggesting that apoptosis could be saturated after a certain dose of UV exposure. Therefore, although we found that the apoptosis triggered by the 50 mJ/cm² UVB dose was not affected by trehalose treatment, the current data did not elicit the conclusion that the trehalose-induced cytoprotective effect observed in UVB-challenged cells was not relevant to apoptosis.

Although Higuchi *et al.* discovered that sucrose-induced autophagy led to the absence of hydrolysis enzymes in mouse embryonic fibroblasts⁶⁶, the mechanism by which trehalose, sucrose and raffinose activate autophagy is unclear. Interestingly, Martinez-Lopez *et al.* reported that ERK phosphorylation was increased by acute trehalose exposure for 2 hours, although prolonged exposure (12 or 24 hours) failed to increase ERK phosphorylation⁷⁴. Their results indicated that trehalose-induced ERK phosphorylation was dependent on autophagy because ERK phosphorylation was not observed in ATG5^{-/-} mouse embryonic fibroblasts. Moreover, Wei *et al.* found that abrogation of ERK phosphorylation by U0126 did not affect trehalose-induced autophagy⁷⁵. Therefore, ERK, which is closely related to autophagy regulation, does not mediate trehalose-induced autophagy. In a recent promising report by Tanji *et al.*, trehalose treatment increased the expression of several chaperone molecules, including HSP90 and SigmaR1, and Beclin 1 phosphorylation in mice, although the authors did not confirm whether these effects led to autophagy induction⁷⁶. Additionally, He *et al.* reported that trehalose inhibits NF- κ B activation by LPS-mediated stimulation⁷⁷, and NF- κ B activation has been reported to be involved in autophagy regulation⁷⁸. Taken together, these results suggest that the roles of the chaperone molecules, the NF- κ B pathway and the Beclin 1 complex in trehalose-activated autophagy warrant attention in future studies.

Here, our work verified that trehalose, sucrose and raffinose do not affect the activity of mTOR, which is a key regulator of cell metabolism, proliferation and survival, even though autophagy was activated. Indeed, clinical application of mTOR-dependent autophagy inducers, such as rapamycin, must take into account their effect on mTOR inhibition because cellular functions besides autophagy are potentially disturbed⁷⁹. For example, Chaoul N *et al.*⁸⁰ reported that rapamycin affects cancer vaccine therapy by impairing antitumour CD8⁺ T cell responses. Therefore, our findings about trehalose, sucrose and raffinose and their mTOR-independent regulation of autophagy have notable implications for human disease therapy.

Materials and Methods

Cell culture. HaCaT cells (described previously⁸¹), A431 cells and HeLa cells (from the Cell Resource Centre, IBMS, Chinese Academy of Medical Sciences and Peking Union Medical College) were cultured in Dulbecco's modified Eagle's medium (DMEM) supplemented with foetal bovine serum (Gibco, Invitrogen Corp., Carlsbad, CA, USA). Primary human keratinocytes (described previously⁸²) and CCD 1102 KERTr cells (ATCC Number CRL-2310) were cultured in Keratinocyte-SFM Medium (Gibco, Invitrogen Corp., Carlsbad, CA, USA).

Reagents and antibodies. The compounds used in this study included trehalose (T0167), glucose (G8270), sucrose (84097), maltose (M5885), raffinose (R0250), sorbitol (240850), 10 μ g/mL of E64d, 10 μ g/mL of pepstatin, rapamycin, chloroquine, dimethyl sulfoxide, acridine orange (AO, A8097), and thiazolyl blue tetrazolium (M5655) (all from Sigma-Aldrich, St. Louis, MO, USA). Other compounds included wortmannin (Santa Cruz, Dallas, TX, USA), Torin 1 (Tocris, Bristol, UK) and pp242 (abcam, Cambridge, MA, USA). Primary antibodies included anti-LC3A/B (#4108), anti- β -Actin (#8457), anti-mTOR (#2983), anti-phospho-mTOR Ser2481 (#2974), anti-phospho-mTOR Ser2448 (#5536), anti-Raptor (#2280), anti-phospho-Raptor Ser792 (#2083), anti-4E-BP1 (#9644), anti-phospho-4E-BP1 Thr37/46 (#2855), anti-phospho-4E-BP1 Ser65 (#9456), anti-Rictor (#2114), anti-phospho-Rictor Thr1135 (#3806), anti-PKC α (#2056), anti-phospho-PKC α / β II Thr638/641 (#9375), anti-phospho-ULK1 Ser555 (#5869), anti-phospho-ULK1 Ser757 (#6888), anti-ULK1 (#4773), anti-Atg7 (#8558), anti-Atg3 (#3415), anti-Atg5 (#8540), anti-Atg9A (#13509), anti-WIP1 (#12124), anti-WIP2 (#8567), anti-phospho-p70 S6 kinase Thr389 (#9234), anti-phospho-p70 S6 kinase Ser371 (#9208), anti-p70 S6 kinase (#2708), anti-S6 ribosomal protein (#2217), anti-phospho-S6 ribosomal protein Ser240/244 (#5364), anti-phospho-S6 ribosomal protein Ser235/236 (#4858), anti-cleaved PARP Asp214 (#5625) and anti-Caspase-3 (#9665) (all from Cell Signaling Technology, Danvers, MA, USA).

Western blotting. The cells were lysed in RIPA Lysis Buffer containing Protease Inhibitor Cocktail and the phosphatase inhibitor PhosSTOP (both from Roche Applied Science, Basel, Switzerland). The protein concentration of the whole cell lysate was determined by the BCA assay (Beyotime Biotechnology, Haimen, Jiangsu, China). Proteins from the cell lysates were loaded onto 4–15% Mini-PROTEAN TGX precast polyacrylamide gels (Bio-Rad Laboratories, Hercules, CA, USA). Then, the proteins were transferred onto PVDF membranes (Bio-Rad Laboratories). After blocking, the membranes were sequentially incubated with the indicated primary and secondary antibodies (Cell Signaling Technology). The protein bands were visualized using an Immuno-Star WesternC Chemiluminescence Kit (170–5070, Bio-Rad Laboratories) using a chemiluminescence imaging method. The band intensities were quantified using Quantity One. β -Actin or GAPDH served as the loading control. LC3 Control Cell Extracts (#11972) and p70 S6 Kinase Control Cell Extracts (#9203) (Cell Signaling Technology) were used to identify the sensitivity of antibodies, including anti-LC3, anti-phosphorylated mTOR and anti-substrates of mTOR (Fig. S1a,b).

GFP-LC3B puncta analysis. A transgene for GFP-LC3B or GFP-LC3 (G120A) was transfected into cells using the Premo Autophagy Sensor LC3B-GFP BacMam 2.0 system according to the manufacturer's instructions

(P36235, Invitrogen Corp., Carlsbad, CA, USA). Chloroquine was used to evaluate the sensitivity of human keratinocytes to this system (Fig. S2a). LC3B (G120A)-GFP served as the negative control. Before detection, the cells were transfected for at least 24 hours. Next, cells with or without treatment were imaged using an OLYMPUS FV1000 laser scanning confocal microscope as follows: GFP scanning, $\lambda_{ex} = 530$ nm and $\lambda_{em} = 500$ nm. In all cases, the number of GFP-LC3B puncta per cell was counted using the ImageJ software (<http://imagej.nih.gov/ij/>).

AO staining assay. The AO staining assay was employed to monitor the autophagy process by labelling acidic vesicular organelles (AVO) based on the theory that autophagosomes are vacuole structures that belong to the AVOs. In the AO-stained cells, the nuclei and cytoplasm showed deep green and slight green fluorescence, respectively, whereas the AVOs were marked with red fluorescence. Thus, the intensity of the red fluorescence was proportional to the AVO volume. Comparison of the mean red/green fluorescence ratios per cell between different populations was used to monitor the autophagy level. After treatment, the cells were washed with PBS and incubated with AO (5 μ g/mL for 10 minutes) at room temperature. The cells were imaged using a laser scanning confocal microscope (AO G: $\lambda_{ex} = 488$ nm and $\lambda_{em} = 515$ nm; AO R: $\lambda_{ex} = 546$ nm and $\lambda_{em} = 620$ nm). The red and green fluorescence intensities in the cells were determined by Quantity One. The red/green fluorescence ratios for individual cells in three independent experiments were used to determine the mean and the statistical significance of the differences was analysed^{17,37,38}. Rapamycin and wortmannin treatment and Earle's balanced salt solution (EBSS, used for nutrient starvation) incubation were used to confirm the sensitivity of this assay for monitoring autophagy regulation in human keratinocytes (Fig. S2B).

Lactate dehydrogenase (LDH) assay. The LDH assay was employed to evaluate cell death based on the idea that LDH would be released from the cytoplasm through the damaged plasma membrane when cell death occurred⁴⁶. As a result, quantification of the LDH level in cell culture supernatants was used to evaluate cell death in our study with an LDH cytotoxicity assay detection kit (Beyotime Biotechnology) according to the manufacturer's instructions. Briefly, HaCaT cells were treated with or without 50 mJ/cm² UVB radiation; then, the cells were cultured in the presence or absence of 100 mM trehalose for 12 hours. Cell culture supernatants were collected for measurement. The optical density was measured at a 490 nm wavelength. The percentage of cell death was calculated with the formula: Cytotoxicity level (percentage of cell death) = (OD of experimental release (trehalose treatment, UVB exposure, or trehalose treatment after UVB exposure, respectively) - OD of spontaneous release (cell with normal culture))/(OD of maximum release (cells treated with LDH releasing reagent provided in kit) - OD of spontaneous release (cell with normal culture)).

Trypan blue staining. HaCaT cells were treated with or without 50 mJ/cm² UVB radiation; then, the cells were cultured in the presence or absence of 100 mM trehalose for 12 or 24 hours. Subsequently, the cells were digested and stained using a Trypan blue staining cell viability assay kit (Beyotime Biotechnology) to assess cell viability in a blood cell counting chamber according to the manufacturer's instructions⁴⁷. The percentage of surviving cells = (total number of cells - number of trypan blue positive cells)/total number of cells.

Colony formation assay. HaCaT cells were treated with or without 50 mJ/cm² UVB radiation; then, the cells were cultured in the presence or absence of 100 mM trehalose for 12 hours. Subsequently, the different groups of cells were seeded into 6 cm tissue culture dishes with 800 cells per dish in 6 ml of DMEM. After culture for 10 days at 37 °C, the cells were washed with warm PBS and fixed in 100% methanol for 5 minutes. Then, the cells were Giemsa stained for 10 minutes to visualize the cell colonies. A colony was defined as a cluster of more than 20 cells. The images were acquired using a Canon EOS 100D digital camera. We conducted the colony formation assay in triplicate to assess the statistical significance.

UVB radiation. UV light between 290 and 320 nm with a peak at 310 nm was delivered by a UVB irradiation apparatus with a UVB lamp (Philips UVB Broadband PL-S 9W/12). The irradiance was 1.50 mW/cm² at a distance of 16 cm. The cells were irradiated for 6.7, 33.3 or 50 seconds at the 10, 50 or 75 mJ/cm² exposure doses. After irradiation, the cells were incubated with fresh medium with or without trehalose.

Annexin V-EGFP Apoptosis Detection. Apoptotic HaCaT cells were identified using an Annexin V-EGFP Apoptosis Detection Kit (Beyotime Biotechnology). After treatment, the cells were incubated with Annexin-EGFP and propidium iodide (PI). The membranes of the apoptotic cells were stained with Annexin-EGFP. The nuclei of non-viable apoptotic cells were stained with PI accompanied by the Annexin-EGFP staining. The cells were imaged using a laser scanning confocal microscope. The percentage of apoptotic cells was calculated from three independent experiments and the statistical significance of the differences was analysed.

Statistical Analysis. The independent experiments were performed at different times. Similar results were obtained from at least three independent experiments for the statistical analysis. The data were analysed by univariate ANOVA or Student's t-test. Statistical significance was identified as a *P* value of less than 0.05.

References

1. Chen, Q. & Haddad, G. G. Role of trehalose phosphate synthase and trehalose during hypoxia: from flies to mammals. *J Exp Biol* **207**, 3125–9, doi: 10.1242/jeb.01133 (2004).
2. Yamaguchi, R. *et al.* Mitochondria frozen with trehalose retain a number of biological functions and preserve outer membrane integrity. *Cell Death Differ* **14**, 616–24, doi: 10.1038/sj.cdd.4402035 (2007).
3. Corradini, D., Strelakova, E. G., Stanley, H. E. & Gallo, P. Microscopic mechanism of protein cryopreservation in an aqueous solution with trehalose. *Sci Rep* **3**, 1218 (2013).

4. Cejkova, J. *et al.* Reduced UVB-induced corneal damage caused by reactive oxygen and nitrogen species and decreased changes in corneal optics after trehalose treatment. *Histol Histopathol* **25**, 1403–16 (2010).
5. Benaroudj, N., Lee, D. H. & Goldberg, A. L. Trehalose accumulation during cellular stress protects cells and cellular proteins from damage by oxygen radicals. *J Biol Chem* **276**, 24261–7, doi: 10.1074/jbc.M101487200 (2001).
6. Arora, A., Ha, C. & Park, C. B. Inhibition of insulin amyloid formation by small stress molecules. *FEBS Lett* **564**, 121–5, doi: 10.1016/S0014-5793(04)00326-6 (2004).
7. Liu, R., Barkhordarian, H., Emadi, S., Park, C. B. & Sierks, M. R. Trehalose differentially inhibits aggregation and neurotoxicity of beta-amyloid 40 and 42. *Neurobiol Dis* **20**, 74–81, doi: 10.1016/j.nbd.2005.02.003 (2005).
8. Choi, A. M., Ryter, S. W. & Levine, B. Autophagy in human health and disease. *N Engl J Med* **368**, 651–62, doi: 10.1056/NEJMra1205406 (2013).
9. Mizushima, N., Levine, B., Cuervo, A. M. & Klionsky, D. J. Autophagy fights disease through cellular self-digestion. *Nature* **451**, 1069–75, doi: 10.1038/nature06639 (2008).
10. Rubinsztein, D. C., Codogno, P. & Levine, B. Autophagy modulation as a potential therapeutic target for diverse diseases. *Nat Rev Drug Discov* **11**, 709–30, doi: 10.1038/nrd3802 (2012).
11. Mancias, J. D. & Kimmelman, A. C. Targeting autophagy addiction in cancer. *Oncotarget* **2**, 1302–6, doi: 10.18632/oncotarget.384 (2011).
12. Sarkar, S., Davies, J. E., Huang, Z., Tunnacliffe, A. & Rubinsztein, D. C. Trehalose, a novel mTOR-independent autophagy enhancer, accelerates the clearance of mutant huntingtin and alpha-synuclein. *J Biol Chem* **282**, 5641–52, doi: 10.1074/jbc.M609532200 (2007).
13. Castillo, K. *et al.* Trehalose delays the progression of amyotrophic lateral sclerosis by enhancing autophagy in motoneurons. *Autophagy* **9**, 1308–20, doi: 10.4161/auto.25188 (2013).
14. Aguib, Y. *et al.* Autophagy induction by trehalose counteracts cellular prion infection. *Autophagy* **5**, 361–9 (2009).
15. Xu, C., Li, X., Wang, F., Weng, H. & Yang, P. Trehalose prevents neural tube defects by correcting maternal diabetes-suppressed autophagy and neurogenesis. *Am J Physiol Endocrinol Metab* **305**, E667–78, doi: 10.1152/ajpendo.00185.2013 (2013).
16. Rodriguez-Navarro, J. A. *et al.* Trehalose ameliorates dopaminergic and tau pathology in parkin deleted/tau overexpressing mice through autophagy activation. *Neurobiol Dis* **39**, 423–38, doi: 10.1016/j.nbd.2010.05.014 (2010).
17. Klionsky, D. J. *et al.* Guidelines for the use and interpretation of assays for monitoring autophagy. *Autophagy* **8**, 445–544, doi: 10.4161/auto.19496 (2012).
18. Li, Y. *et al.* ZNF32 inhibits autophagy through the mTOR pathway and protects MCF-7 cells from stimulus-induced cell death. *Sci Rep* **5**, 9288, doi: 10.1038/srep09288 (2015).
19. Peng, N. *et al.* An activator of mTOR inhibits oxLDL-induced autophagy and apoptosis in vascular endothelial cells and restricts atherosclerosis in apolipoprotein E(–)/(–) mice. *Sci Rep* **4**, 5519, doi: 10.1038/srep05519 (2014).
20. Ganley, I. G. *et al.* ULK1.ATG13.FIP200 complex mediates mTOR signaling and is essential for autophagy. *J Biol Chem* **284**, 12297–305, doi: 10.1074/jbc.M900573200 (2009).
21. Tan, S. H. *et al.* Induction of autophagy by palmitic acid via protein kinase C-mediated signaling pathway independent of mTOR (mammalian target of rapamycin). *J Biol Chem* **287**, 14364–76, doi: 10.1074/jbc.M111.294157 (2012).
22. Williams, A. *et al.* Novel targets for Huntington's disease in an mTOR-independent autophagy pathway. *Nat Chem Biol* **4**, 295–305, doi: 10.1038/nchembio.79 (2008).
23. Sarkar, S., Ravikumar, B., Floto, R. A. & Rubinsztein, D. C. Rapamycin and mTOR-independent autophagy inducers ameliorate toxicity of polyglutamine-expanded huntingtin and related proteinopathies. *Cell Death Differ* **16**, 46–56, doi: 10.1038/cdd.2008.110 (2009).
24. Fuchs, E. Epidermal differentiation: the bare essentials. *J Cell Biol* **111**, 2807–14 (1990).
25. Aymard, E. *et al.* Autophagy in human keratinocytes: an early step of the differentiation? *Exp Dermatol* **20**, 263–8, doi: 10.1111/j.1600-0625.2010.01157.x (2011).
26. Griffin, L. M., Cicchini, L. & Pyeon, D. Human papillomavirus infection is inhibited by host autophagy in primary human keratinocytes. *Virology* **437**, 12–9, doi: 10.1016/j.virol.2012.12.004 (2013).
27. Murase, D. *et al.* Autophagy has a significant role in determining skin color by regulating melanosome degradation in keratinocytes. *J Invest Dermatol* **133**, 2416–24, doi: 10.1038/jid.2013.165 (2013).
28. Lee, H. M. *et al.* Autophagy negatively regulates keratinocyte inflammatory responses via scaffolding protein p62/SQSTM1. *J Immunol* **186**, 1248–58, doi: 10.4049/jimmunol.1001954 (2011).
29. Suksee, S. *et al.* Targeted deletion of Atg5 reveals differential roles of autophagy in keratin K5-expressing epithelia. *Biochem Biophys Res Commun* **430**, 689–94, doi: 10.1016/j.bbrc.2012.11.090 (2013).
30. Rossiter, H. *et al.* Epidermal keratinocytes form a functional skin barrier in the absence of Atg7 dependent autophagy. *J Dermatol Sci* **71**, 67–75, doi: 10.1016/j.jdermsci.2013.04.015 (2013).
31. Yoshihara, N. *et al.* The significant role of autophagy in the granular layer in normal skin differentiation and hair growth. *Arch Dermatol Res* **307**, 159–69, doi: 10.1007/s00403-014-1508-0 (2015).
32. Soma-Nagae, T. *et al.* The lysosomal signaling anchor p18/LAMTOR1 controls epidermal development by regulating lysosome-mediated catabolic processes. *J Cell Sci* **126**, 3575–84, doi: 10.1242/jcs.121913 (2013).
33. Wang, R. C. & Levine, B. Calcipotriol induces autophagy in HeLa cells and keratinocytes. *J Invest Dermatol* **131**, 990–3, doi: 10.1038/jid.2010.423 (2011).
34. Tong, X., Smith, K. A. & Pelling, J. C. Apigenin, a chemopreventive bioflavonoid, induces AMP-activated protein kinase activation in human keratinocytes. *Mol Carcinog* **51**, 268–79, doi: 10.1002/mc.20793 (2012).
35. Dong, Q. *et al.* Efavirenz induces autophagy and aberrant differentiation in normal human keratinocytes. *Int J Mol Med* **31**, 1305–12, doi: 10.3892/ijmm.2013.1327 (2013).
36. Vitale, N. *et al.* Resveratrol couples apoptosis with autophagy in UVB-irradiated HaCaT cells. *PLoS One* **8**, e80728, doi: 10.1371/journal.pone.0080728 (2013).
37. Paglin, S. *et al.* A novel response of cancer cells to radiation involves autophagy and formation of acidic vesicles. *Cancer Res* **61**, 439–44 (2001).
38. De Amicis, F. *et al.* Bergapten drives autophagy through the up-regulation of PTEN expression in breast cancer cells. *Mol Cancer* **14**, 130, doi: 10.1186/s12943-015-0403-4 (2015).
39. Kabeya, Y. *et al.* LC3, a mammalian homologue of yeast Apg8p, is localized in autophagosome membranes after processing. *EMBO J* **19**, 5720–8, doi: 10.1093/emboj/19.21.5720 (2000).
40. Zhang, X. *et al.* mTOR-independent, autophagic enhancer trehalose prolongs motor neuron survival and ameliorates the autophagic flux defect in a mouse model of amyotrophic lateral sclerosis. *Autophagy* **10**, 588–602, doi: 10.4161/auto.27710 (2014).
41. Kim, B. R. *et al.* The anti-tumor activator sMEK1 and paclitaxel additionally decrease expression of HIF-1alpha and VEGF via mTORC1-S6K/4E-BP-dependent signaling pathways. *Oncotarget* **5**, 6540–51, doi: 10.18632/oncotarget.2119 (2014).
42. Dibble, C. C., Asara, J. M. & Manning, B. D. Characterization of Rictor phosphorylation sites reveals direct regulation of mTOR complex 2 by S6K1. *Mol Cell Biol* **29**, 5657–70, doi: 10.1128/MCB.00735-09 (2009).
43. Guo, F. *et al.* mTOR regulates DNA damage response through NF-kappaB-mediated FANCD2 pathway in hematopoietic cells. *Leukemia* **27**, 2040–6, doi: 10.1038/leu.2013.93 (2013).
44. Francipane, M. G. & Lagasse, E. Selective targeting of human colon cancer stem-like cells by the mTOR inhibitor Torin-1. *Oncotarget* **4**, 1948–62, doi: 10.18632/oncotarget.1310 (2013).

45. Bhui, K. *et al.* Bromelain inhibits nuclear factor kappa-B translocation, driving human epidermoid carcinoma A431 and melanoma A375 cells through G(2)/M arrest to apoptosis. *Mol Carcinog* **51**, 231–43, doi: 10.1002/mc.20769 (2012).
46. Sun, B. *et al.* The nonstructural protein NP1 of human bocavirus 1 induces cell cycle arrest and apoptosis in HeLa cells. *Virology* **440**, 75–83, doi: 10.1016/j.virol.2013.02.013 (2013).
47. Chen, H., Ma, N., Xia, J., Liu, J. & Xu, Z. beta2-Adrenergic receptor-induced transactivation of epidermal growth factor receptor and platelet-derived growth factor receptor via Src kinase promotes rat cardiomyocyte survival. *Cell Biol Int* **36**, 237–44, doi: 10.1042/CBI20110162 (2012).
48. Tyagi, N. *et al.* Development and Characterization of a Novel *in vitro* Progression Model for UVB-Induced Skin Carcinogenesis. *Sci Rep* **5**, 13894, doi: 10.1038/srep13894 (2015).
49. Douroudis, K. *et al.* Polymorphisms in the ATG16L1 gene are associated with psoriasis vulgaris. *Acta Derm Venereol* **92**, 85–7, doi: 10.2340/00015555-1183 (2012).
50. Douroudis, K. *et al.* ATG16L1 gene polymorphisms are associated with palmoplantar pustulosis. *Hum Immunol* **72**, 613–5, doi: 10.1016/j.humimm.2011.03.009 (2011).
51. Jeong, T. J. *et al.* Association of UVRAG polymorphisms with susceptibility to non-segmental vitiligo in a Korean sample. *Exp Dermatol* **19**, e323–5, doi: 10.1111/j.1600-0625.2009.01039.x (2010).
52. Buckingham, E. M. *et al.* Autophagic flux without a block differentiates varicella-zoster virus infection from herpes simplex virus infection. *Proc Natl Acad Sci USA* **112**, 256–61, doi: 10.1073/pnas.1417878112 (2015).
53. Grose, C. Autophagy during common bacterial and viral infections of children. *Pediatr Infect Dis J* **29**, 1040–2, doi: 10.1097/INF.0b013e3181e77f43 (2010).
54. Sivridis, E. *et al.* LC3A-positive “stone-like” structures in cutaneous squamous cell carcinomas. *Am J Dermatopathol* **33**, 285–90, doi: 10.1097/DAD.0b013e3181f10de0 (2011).
55. Zhang, L., Zhang, J., Chen, L. & Wang, J. Autophagy in human skin squamous cell carcinoma: Inhibition by 3-MA enhances the effect of 5-FU-induced chemotherapy sensitivity. *Oncol Rep* **34**, 3147–55, doi: 10.3892/or.2015.4302 (2015).
56. Boos, W. *et al.* Trehalose transport and metabolism in *Escherichia coli*. *J Bacteriol* **172**, 3450–61 (1990).
57. Elbein, A. D., Pan, Y. T., Pastuszak, I. & Carroll, D. New insights on trehalose: a multifunctional molecule. *Glycobiology* **13**, 17R–27R, doi: 10.1093/glycob/cwg047 (2003).
58. Ravikumar, B. *et al.* Raised intracellular glucose concentrations reduce aggregation and cell death caused by mutant huntingtin exon 1 by decreasing mTOR phosphorylation and inducing autophagy. *Hum Mol Genet* **12**, 985–94, doi: 10.1093/hmg/ddg109 (2003).
59. Wang, X. Y. *et al.* High glucose environment inhibits cranial neural crest survival by activating excessive autophagy in the chick embryo. *Sci Rep* **5**, 18321, doi: 10.1038/srep18321 (2015).
60. Spravchikov, N. *et al.* Glucose effects on skin keratinocytes: implications for diabetes skin complications. *Diabetes* **50**, 1627–35, doi: 10.2337/diabetes.50.7.1627 (2001).
61. DeBosch, B. J. *et al.* Trehalose inhibits solute carrier 2A (SLC2A) proteins to induce autophagy and prevent hepatic steatosis. *Sci Signal* **9**, ra21, doi: 10.1126/scisignal.aac5472 (2016).
62. Hinch, D. K., Zuther, E., Hellwege, E. M. & Heyer, A. G. Specific effects of fructo- and gluco-oligosaccharides in the preservation of liposomes during drying. *Glycobiology* **12**, 103–10, doi: 10.1093/glycob/12.2.103 (2002).
63. Seglen, P. O., Overbye, A. & Saetre, F. Sequestration assays for mammalian autophagy. *Methods Enzymol* **452**, 63–83, doi: 10.1016/S0076-6879(08)03605-7 (2009).
64. Seglen, P. O., Gordon, P. B., Tolleshaug, H. & Hoyvik, H. Use of [3H]raffinose as a specific probe of autophagic sequestration. *Exp Cell Res* **162**, 273–7 (1986).
65. Klionsky, D. J., Cuervo, A. M. & Seglen, P. O. Methods for monitoring autophagy from yeast to human. *Autophagy* **3**, 181–206, doi: 10.4161/auto.3678 (2007).
66. Higuchi, T., Nishikawa, J. & Inoue, H. Sucrose induces vesicle accumulation and autophagy. *J Cell Biochem* **116**, 609–17, doi: 10.1002/jcb.25012 (2015).
67. Matsumura, Y. & Ananthaswamy, H. N. Toxic effects of ultraviolet radiation on the skin. *Toxicol Appl Pharmacol* **195**, 298–308, doi: 10.1016/j.taap.2003.08.019 (2004).
68. Lee, H. S. *et al.* A systems-biological study on the identification of safe and effective molecular targets for the reduction of ultraviolet B-induced skin pigmentation. *Sci Rep* **5**, 10305, doi: 10.1038/srep10305 (2015).
69. Cao, G. *et al.* EGCG protects against UVB-induced apoptosis via oxidative stress and the JNK1/c-Jun pathway in ARPE19 cells. *Mol Med Rep* **5**, 54–9, doi: 10.3892/mmr.2011.582 (2012).
70. Zaid, M. A., Afaq, F., Syed, D. N., Dreher, M. & Mukhtar, H. Inhibition of UVB-mediated oxidative stress and markers of photoaging in immortalized HaCaT keratinocytes by pomegranate polyphenol extract POMx. *Photochem Photobiol* **83**, 882–8, doi: 10.1111/j.1751-1097.2007.00157.x (2007).
71. Hedrych-Ozimina, A. *et al.* Enhanced contact allergen- and UVB-induced keratinocyte apoptosis in the absence of CD95/Fas/Apo-1. *Cell Death Differ* **18**, 155–63, doi: 10.1038/cdd.2010.83 (2011).
72. Mallikarjuna, G., Dhanalakshmi, S., Singh, R. P., Agarwal, C. & Agarwal, R. Silibinin protects against photocarcinogenesis via modulation of cell cycle regulators, mitogen-activated protein kinases, and Akt signaling. *Cancer Res* **64**, 6349–56, doi: 10.1158/0008-5472.CAN-04-1632 (2004).
73. Ito, S. *et al.* GADD34 inhibits activation-induced apoptosis of macrophages through enhancement of autophagy. *Sci Rep* **5**, 8327, doi: 10.1038/srep08327 (2015).
74. Martinez-Lopez, N., Athonvarankul, D., Mishall, P., Sahu, S. & Singh, R. Autophagy proteins regulate ERK phosphorylation. *Nat Commun* **4**, 2799, doi: 10.1038/srep08327 (2013).
75. Wei, P. F. *et al.* Differential ERK activation during autophagy induced by europium hydroxide nanorods and trehalose: Maximum clearance of huntingtin aggregates through combined treatment. *Biomaterials* **73**, 160–74, doi: 10.1038/srep08327 (2015).
76. Tanji, K. *et al.* Trehalose intake induces chaperone molecules along with autophagy in a mouse model of Lewy body disease. *Biochem Biophys Res Commun* **465**, 746–52, doi: 10.1016/j.bbrc.2015.08.076 (2015).
77. He, Q. *et al.* Trehalose alleviates PC12 neuronal death mediated by lipopolysaccharide-stimulated BV-2 cells via inhibiting nuclear transcription factor NF-kappaB and AP-1 activation. *Neurotox Res* **26**, 430–9, doi: 10.1007/s12640-014-9487-7 (2014).
78. Liu, S. *et al.* NF-kappaB activation was involved in reactive oxygen species-mediated apoptosis and autophagy in 1-oxo-oedesm-11(13)-eno-12,8alpha-lactone-treated human lung cancer cells. *Arch Pharm Res* **37**, 1039–52, doi: 10.1007/s12272-013-0270-8 (2014).
79. Soll, C. & Clavien, P. A. Inhibition of mammalian target of rapamycin: the janus face of immunosuppression? *Hepatology* **51**, 1113–5, doi: 10.1002/hep.23582 (2010).
80. Chaoul, N. *et al.* Rapamycin impairs antitumor CD8+ T cell responses and vaccine-induced tumor eradication. *Cancer Res* **75**, 3279–91, doi: 10.1158/0008-5472.CAN-15-0454 (2015).
81. Tu, H. Q. *et al.* Effects of tacrolimus on IFN-gamma signaling in keratinocytes: possible mechanisms by which tacrolimus affects IFN-gamma-dependent skin inflammation. *Eur J Dermatol* **21**, 22–31, doi: 10.1684/ejd.2011.1154 (2011).
82. Li, M., Chen, Q., Shen, Y. & Liu, W. Candida albicans phospholipomannan triggers inflammatory responses of human keratinocytes through Toll-like receptor 2. *Exp Dermatol* **18**, 603–10, doi: 10.1111/j.1600-0625.2008.00832.x (2009).

Acknowledgements

This work was supported by grants from the National Natural Science Foundation of China (No. 81171513, 81371755), the PhD Programs Foundation of Ministry of Education of China (No. 20111106110041, 20131106120046), the Jiangsu Provincial Special Program of Medical Science (BL2012003) and the Jiangsu Province Natural Science Foundation (No. BK20131064) to Heng Gu. Xu Chen and Song Xu are supported by the PUMC Youth Fund and Fundamental Research Funds for the Central Universities (3332014008, 3332015026).

Author Contributions

X.C. and M.L. wrote the main manuscript text, and contributed equally to this work. X.C., L.L., S.X., D.H. and M.J. jointly performed the experiments, prepared all figures and performed statistical analysis in this work. J.H. supervised the experimental design and revised manuscript text. H.G. and K.C. are the corresponding authors. All authors reviewed the manuscript.

Additional Information

Supplementary information accompanies this paper at <http://www.nature.com/srep>

Competing financial interests: The authors declare no competing financial interests.

How to cite this article: Chen, X. *et al.* Trehalose, sucrose and raffinose are novel activators of autophagy in human keratinocytes through an mTOR-independent pathway. *Sci. Rep.* **6**, 28423; doi: 10.1038/srep28423 (2016).



This work is licensed under a Creative Commons Attribution 4.0 International License. The images or other third party material in this article are included in the article's Creative Commons license, unless indicated otherwise in the credit line; if the material is not included under the Creative Commons license, users will need to obtain permission from the license holder to reproduce the material. To view a copy of this license, visit <http://creativecommons.org/licenses/by/4.0/>